Case Studies in Thermal Engineering 51 (2023) 103606

Contents lists available at ScienceDirect

Case Studies in Thermal Engineering

journal homepage: www.elsevier.com/locate/csite

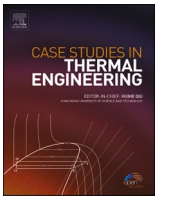

Evidence-based numerical building model enhancement and building energy efficiency evaluation in the case of Morocco

Niima Es-sakali [a,b,*], Samir Idrissi Kaitouni [b,c], Imad Ait Laasri [b,d], Mohamed Oualid Mghazli [b,e,f], Moha Cherkaoui [a], Moritz Bühler [g], Jens Pfafferott [g]

[a] LMAID laboratory, Rabat National School of Mines, 10070, Rabat, Morocco
[b] Green Energy Park (IRESEN, UM6P), 43150, Benguerir, Morocco
[c] Faculty of Science and Technology, Abdelmalek Essaadi University, B.P. 416 Tangier, Tétouan, Morocco
[d] Laboratory (LaMEE), Faculty of Sciences Semlalia, Cadi Ayyad University, Marrakesh, Morocco
[e] Univ Lyon, ENTPE, Ecole Centrale de Lyon, CNRS, LTDS, UMR 5513, 69518, Vaulx-en-Velin Cedex, France
[f] Civil Engineering Laboratory, Mohammadia School of Engineers, Mohammed V University in Rabat, Morocco
[g] Institute of Sustainable Energy Systems (INES), Offenburg University of Applied Sciences, Offenburg, Germany

HIGHLIGHTS

- A numerical building validation enhancement strategy was conducted on a lightweight building.
- Evidence-based data were collected from 3 in-situ building measurements.
- The impact of building parameters on the accuracy of the energy model is studied.
- The energy use of the lightweight construction with the VRF system was assessed in 12 Moroccan regions.

ARTICLE INFO

Keywords:
Building energy model
Variable refrigerant flow system
Light-weight building
Energy simulation

ABSTRACT

This paper presents a framework for numerical building validation enhancement based on detailed building specifications from in-situ measurements and evidence-based validation assessment undertaken on a detached sustainable lightweight building in a semi-arid climate. The validation process has been undergone in a set of controlled experiments – a free-float period, and steady-state internal temperatures. The validation was conducted for a complete year with a 1-min time step for the hourly indoor temperature and the variable refrigerant flow (VRF) energy consumption. The initial baseline model was improved by three series of validation steps per three different field measurements including thermal transmittance, glazing thermal and optical properties, and airtightness. Then, the accurate and validated model was used for building energy efficiency assessment in 12 regions of Morocco. This study aims to assess the effect of accurate building characteristics values on the numerical model enhancement. The initial CV(RMSE) and NMBE have improved respectively from 14.58 % and −11.23 %–7.85 % and 1.86 % for the indoor temperature. Besides, from 31.17 % to 14.37 %–20.57 % and 9.77 % for energy consumption. The findings demonstrate that the lightweight construction with the use of a variable refrigerant flow system could be energy efficient in the southern regions of Morocco.

* Corresponding author. LMAID laboratory, Rabat National School of Mines, 10070, Rabat, Morocco.
E-mail addresses: niima.essakali@enim.ac.ma, es-sakali@greenenergypark.ma (N. Es-sakali).

https://doi.org/10.1016/j.csite.2023.103606
Received 25 July 2023; Received in revised form 29 September 2023; Accepted 7 October 2023
Available online 14 October 2023

Nomenclature

ECM	Energy conservation measures
BES	Building energy simulation
HVAC	Heating, Ventilation, and air conditioning
ASHRAE	American Society of Heating, Refrigerating, and Air Conditioning Engineers
RMSE	Root Mean Square Error
CV(RMSE)	Coefficient of Variation of RMSE
NMBE	Normalized Mean Bias Error
BEM	Building Energy Model
IPMVP	International Performance Measurement and Verification Protocol
FEMP	Federal Energy Management Program
ACH	Air change per hour
VRF	Variable Refrigerant Flow
OSB	Oriented Strand Board
XPS	Extruded Polystyrene Foam
COP	Coefficient of performance
EER	Energy Efficiency Ratio
HFM	Heat Flow Meter
SHGC	Solar Heat Gain Coefficient
VLT	Visible Light Transmission
$\bar{y}$	The arithmetic Mean of the sample of n observations
$\hat{y}$	Regression model's predicted value of y

1. Introduction

Buildings account for over one-third of the global energy consumption and 40 % of the global CO_2 emissions, making them one of the key sectors influencing energy use and greenhouse gas emissions [1]. Buildings consume approximately 80 % of the total energy used during building operation to ensure indoor comfort temperatures [2]. Therefore, integrating Energy Conservation Measures (ECM) in office buildings can save 30 % of the thermal energy and 13 % of the electrical energy required for regular operation [3]. Building Energy Simulation (BES) is widely used as a decision tool to assist building professionals in the design phase by integrating Heating, Ventilation, and Air Conditioning (HVAC) systems specifications, PV properties, and building envelope characteristics. This contributes to a better understanding of building behavior concerning the capacity for energy production and consumption as well as indoor thermal comfort. Therefore, BES was successfully adopted in the building sector due to its various benefits, such as evaluating energy systems' performance without recurring experimental measurements and setups. This technique helps also in studying the enormous ECM before being implemented in real buildings at very low costs and without consuming much time compared with traditional tools for improving the building energy efficiency. Furthermore, the BES validation is used as the basis for numerous research fields including the prediction of energy use and demand [4–6], application of predictive model control approaches [7,8], development of passive building strategies [9] and the integration of phase change materials in buildings [10,11] or even the application of predictive maintenance strategies for the building energy systems [12,13], as they all need building validation. However, despite the useful pros of BES, it is crucial to consider the minor inconveniences of this technique related to the accuracy of the virtual reproduction of real buildings. This is generally due to the discrepancies and divergencies between measured and simulated results. Many studies in the literature have addressed this issue by detecting differences between simulated and measured results [14–17]. As a result, a building energy model's consistency depends on how closely the simulation results match actual observed data, which is in turn dependent on how reliable the input data is [16]. The accuracy of the predicted and generated data is then enhanced using energy model calibration in comparison to the actual measured data. Generally speaking, two factors affect the accuracy of output data which are the inaccurate input data, such as the thermal properties of building envelope materials, and the simplicity of the building energy model including its energy systems specifications, and HVAC systems schedules [18]. According to ASHRAE Guidelines 14 [19], calibration is defined as a technique that serves to decrease the uncertainty of the predicted or simulated output of the

Table 1
Acceptable margins for validating building energy models.

Calibration Interval	Indices	ASHRAE Guide 14 [19]	IMPVP [20]	FEMP [21]
Monthly	$NMBE_{Monthly}$	±5%	20 %	5 %
	$CV(RMSE)_{Monthly}$	15 %	–	15 %
Hourly	$NMBE_{Hourly}$	±10 %	5 %	10 %
	$CV(RMSE)_{Hourly}$	30 %	20 %	30 %

model by comparing this predicted data with the real measured data under the same circumstances. The accuracy is measured according to some uncertainty indices, such as CV(RMSE) and NMBE statistical indices (Table 1) given by ASHRAE Guide 14 [19], IPMVP [20] and FEMP [21].

Coakley et al. have reviewed in their study [22] the main existing approaches for the development of a BEM calibration framework. These approaches could be generally classified either among automated or manual-based calibration techniques. The automated-based calibration methods depend on developing a mathematical and statistical program that automatically applies the model calibration. The manual-based calibration approaches are the traditional calibration methods used by applying manual iterative BEMs based on expert knowledge by changing building parameters. One of the most popular techniques for automated BEM calibration is the optimization-based calibration technique [23–30]. Finding the output simulation that matches the actual observed data the best and most closely is the aim of optimization techniques. The objective functions of the calibration statistical indices are minimized to achieve calibration optimization. The ability of the optimization-based methodologies to examine all BEM scenarios based on changes in the building's relative factors and building energy system requirements has demonstrated their reliability. Even with their many benefits, these strategies nonetheless have drawbacks that should be seriously taken into consideration before their application. The deployment of optimization-based strategies is costly as well as time-consuming. Depending on the BEM simulation's chosen timestep, it can take several hours or days to establish the simulation of the optimization programs. Moreover, the simulations need to be run on advanced expensive workstations. Furthermore, the results obtained from the automated-based methods are mathematically and statistically correct since they respect the mathematical program developed. Hence, in reality, they could not always match the existing physics of the building. Therefore, manual-based calibration approaches and evidence-based calibration approaches are very common and up to date are still widely used in the literature [31–33].

Moreover, one of the most crucial factors in the BEM validation process is the calibration period. The majority of the conducted research has focused on applying the calibration method for brief times like days, weeks, or even single months [34–38]. However, only a few researchers [39,40] have opted to carry out the calibration process on an entire calendar year of data. The time step of the BEM simulation is also essential for obtaining accurate results. As a result, decreasing the time step increases the accuracy of the simulation results. Nearly all studies, including those conducted by Pachano et al. [41] and Sakiyama et al. [42] have used a 10-min time step to increase accuracy and shorten simulation times. Whereas, others like Cacabelos et al. [43] and Dong et al. [44] have used a 5-min time step. So, in general, the majority of researchers are working with BEM simulation timesteps between one and 10 min, based on the recommendation of EnergyPlus's guidelines [45]. Furthermore, the envelope characteristics are also crucial factors that affect the BEM simulation results. According to the literature [46], the most common parameters that cause differences between measured and real values are the thermal conductivities of the building's opaque and glazing materials, as well as the building's airtightness along with the performance curves of the HVAC systems. So, measuring the real values of each building's parameter is important. For instance, the thermal transmittance varies by several factors including the material's operating years. Weather circumstances have an impact as well; a material's thermal transmittance will vary if it is exposed to too much rain or sun. Besides, the U-value is impacted by post-occupancy as well as the maintenance level. As a result, after a few years of use, the initial value of the thermal transmittance of materials should be confirmed. Furthermore, building infiltration is also another important factor that influences the BEM results. Thus, Ascione et al. [47], have supposed a fixed value of 0.3 ACH for the infiltration. Whereas, Mastouri et al. [48] have used a fixed value of 0.5 ACH, which respects the allowable ranges of infiltration that affect the indoor thermal comfort level according to ASHRAE 62.1 [49] and ASHRAE 62.2 [50]. In that sense, none of the aforementioned researchers has performed an experimental study to confirm the actual values of the building envelope's thermal transmittance, glazing properties, and airtightness values. They have focused directly on the calibration based on sensitivity analysis [51]. Otherwise, a limited number of studies have used a blower door test to confirm the airtightness of their buildings, even though building infiltration is another important factor that influences the BEM results.

Therefore, the main aim of this paper is to develop a detailed and comprehensive building evidence-based validation strategy based on experimental measurements of the key building parameters that affect the BES results, for uncommon existing building construction, the lightweight construction with VRF heat pump system located in the semi-arid climate of Morocco. The input parameters of the BEM are extracted from experimental setups conducted for the thermal transmittance and conductivity of the building envelope, the glazing thermal and optical windows properties, and finally, the building airtightness based on a blower door test. Furthermore, an energy evaluation was carried out on the validated model in 12 Moroccan regions, to assess the energy efficiency of the lightweight construction in different climate zones. Hence, to fill in the major gaps found in the literature, the novelty of the conducted study relies on addressing the following issues;

- Due to the rarity of extended periods of building validation in the literature, the proposed study is based on a full year of data. The calibration was conducted on hourly VRF energy consumption during cooling and heating periods as well as hourly indoor air temperature data for each month according to ASHRAE Guide 14 tolerances.
- As the suggested timesteps for developing simulations are less than 10 min, the minimum time step allowed for the BEM simulation, which is a 1-min timestep, is used to have the highest level of model accuracy and precision. Controversy to literature studies which use 5–10 min timestep.
- The gap in the literature where authors develop their BEMs purely based on technical surveys as well as numerical assumptions without carrying out experimental setups served as the motivation for this research. The developed methodology is based on three sets of in-situ and laboratory experimental tests for the creation and validation of the BEM.
- Due to the lack of literature on experimental studies on lightweight constructions in semi-arid climate. Especially the lack of studies on lightweight real building cases with VRF systems, that can be used as data for building numerical validations. Therefore, this

evidence-based methodology is conducted in the semi-arid environment of Morocco to expand the validation methods applied in such construction and climate, which will provide researchers with enormous data for numerical validations in this field.

The rest of this paper is organized as follows; *Section 2* presents and explains the developed methodology including the building description, the data collection procedure, meteorological data measurement as well as the numerical model development, enhancement, and evaluation. *Section 3* provides an overview of the main findings and discussions obtained from the proposed methodology. *Section 4* provides an overall overview on the potential building improvement in Morocco. *Section 5* summarizes the main conclusions of the conducted study as well as a depth insight into future work and perspectives along with the main recommendations deducted from the paper.

2. Methodology

2.1. Building description

The building utilized in this research (Fig. 1) is a brand-new building constructed in 2019 with a northwest-facing orientation. The structure is situated in Benguerir city in Morocco in the Research & Development platform of Green and Smart Building Park (GSBP). It is a two-story structure with a 3 m-high ceiling and a 92 m^2 total gross roof space (Fig. 2). The building is a sustainable lightweight construction mainly built from wood. As presented in Table 2, the building is insulated with extruded polystyrene foam (XPS), acrylic, and roof waterproofing. The choice of the case study building was based on the building construction type naming lightweight construction, which an is unusual construction type in Morocco. As well as the energy system technology existing in the building. This study evaluates two crucial rooms among the thermal zones existing in the building. Therefore, the building is equipped with two temperature sensors located in rooms 1 & 2. Room 1 is positioned eastward as opposed to room 2, which is facing west. As a result, room 1 receives direct solar radiation in the morning. However, room 2 is protected from the sun's rays in the evenings, by a nearby structure. In addition, room 1 is beneath the first floor as opposed to room 2, which is situated beneath a terrace in a protruding corner of the building. Thus, room 1 experiences greater temperature changes than room 2.

To cover the heating and cooling needs, the building is equipped with a VRF heat pump system. It is a multi-zone direct expansion heating and cooling system containing one single outdoor unit, that supplies several indoor units with small refrigeration tubes. Indoor heat pump units provide hot or cold air using steam compression cycle technology. In cooling mode, the air is drawn into and recycled in the conditioned zone where each unit is located. The function of the compressor/condenser unit is to reject heat outdoors (cooling period) or to absorb heat indoors (heating period). GREE's GMV-140WL/C-T was used as the VRF heat pump system for the studied building. With an energy efficiency ratio (EER) of 3.9 and a coefficient of performance (COP) of 4.18. This system has a cooling capacity of 14 kW and a heating capacity of 16.5 kW. The conceptual diagram of the building VRF system is shown in Fig. 3.

Regarding the occupancy schedule, from April through October, 5 individuals were occupying the building. The time frame for occupancy is from 9:00 a.m. to 6:00 p.m. During this time, the building's occupants operated it as an office, turning on the HVAC system for cooling during the first halves of April and May and for heating during the first half of September. The only month the HVAC system ran continuously was October. The building was then vacant from November until the end of the year, and the HVAC system was left in the OFF setting the entire time.

In the aim of this study, the considered building was monitored for the whole year of 2021. Then, evidence-based data were collected from several in-situ measurements based on a developed sensitivity analysis conducted on the cooling and heating energy consumption. These measurements include thermal conductivity, optical and thermal glazing properties as well as building airtightness. Afterward, three numerical models were developed. Each model will be fed by each evidence-based data category to assess the impact of each building parameter on the accuracy of the base model results. Then, a verification of the developed models was conducted in Room 2. Finally, an energy evaluation of the lightweight building using the VRF system was assessed in all the regions and climatic zones of Morocco, using the validated model (Fig. 4).

Fig. 1. External view of the studied building.

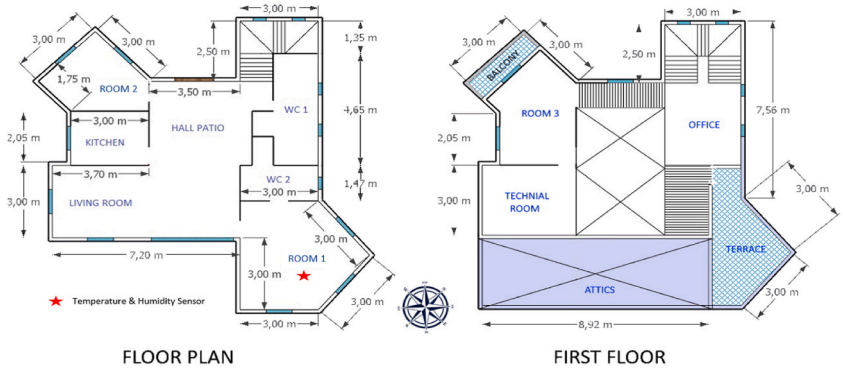

Fig. 2. Studied building plans.

Table 2
Description of the building insulation materials.

	Thickness (mm)	Conductivity (W/m.K)	Application-level
XPS Polystyrene	40	0.034	Walls, roofs & floors
Acrylic	50	0.037	Walls & Ceiling
Cool roofing	1.5	0.026	Roof

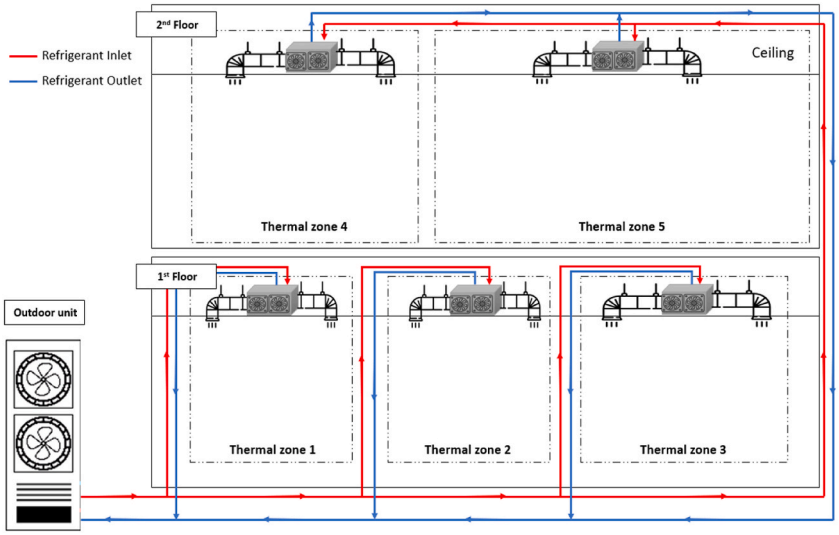

Fig. 3. Conceptual VRF system diagram.

2.2. Evidence-based data collection

The choice of the measured and tested parameters was based on a sensitivity analysis conducted on the cooling and heating energy consumption. The sensitivity analysis presented in Fig. 5 was conducted to detect the building parameters that have the highest influence on the cooling and heating energy consumption. Therefore, these influencing parameters affect also the accuracy of the developed BEM. Thus, before the development of the proposed BEM, it is crucial to conduct a sensitivity analysis with the aim of choosing the building parameters that should be measured, tested, and verified to improve the accuracy of the numerical model. The sensitivity analysis findings have proved that rather than the cooling and heating setpoint temperatures, the infiltration rate, the SHGC, and the thermal conductivity are the most influencing parameters that need to be measured carefully.

2.2.1. In-situ thermal conductivity measurement

The building dimensions, construction, and insulation materials were collected from the building design specifications. The building thermal transmittance was measured using two different methods, the first measurement was conducted using GreenTEG logger device, while the second measurement was conducted using HFM 446 lambda. These two measurement results are compared to the theoretical values to determine the thermal transmittance values that were accurately measured. At the first level, the thermal

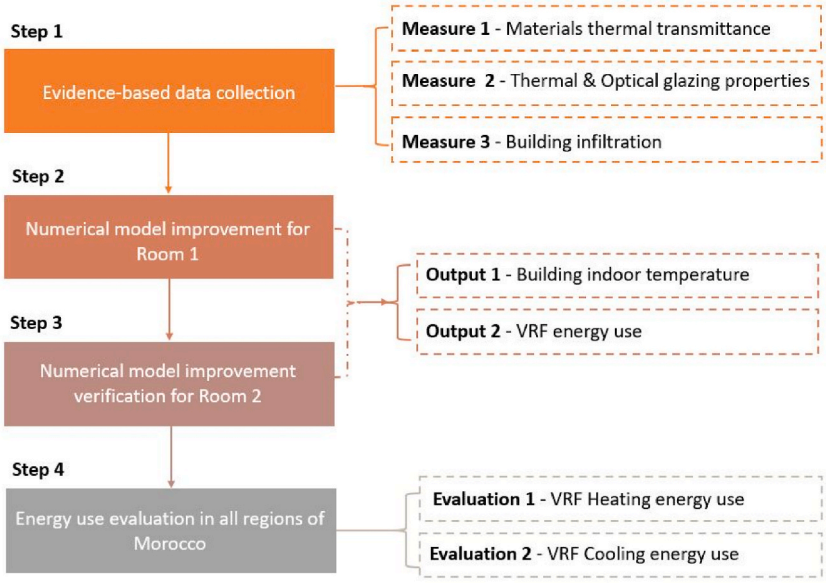

Fig. 4. Proposed methodology.

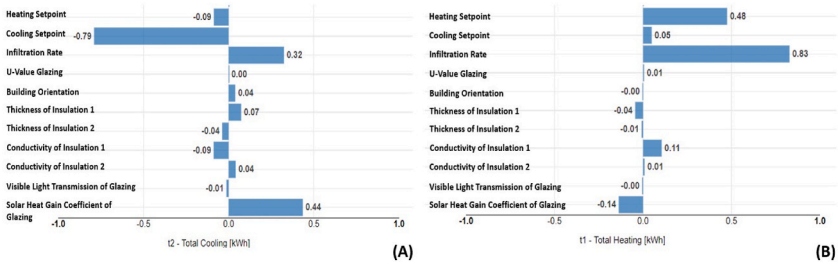

Fig. 5. Sensitivity analysis; (a) for cooling energy use and (b) for heating energy use.

conductivity of the construction and insulation materials was verified using the GreenTEG logger heat flow meter as shown in Fig. 6. The measurement of U-value using this device respects the regulations of ISO9869–1:2014 [52]. Thus, the data acquisition interval was 10 min to meet the regulation. The U-value test measurement was undertaken for 72 h for each test. The location of the heat flux was chosen at a considerable distance from thermal bridges and the HVAC system's direct air supply grills. During the test measurement, a specific shadow was cast around the outside temperature sensor to shield it from direct sunlight. Besides, four in-situ thermal conductivity measurements were conducted on the external wall of the building. Then, the average of these measurements was compared to the theoretical values.

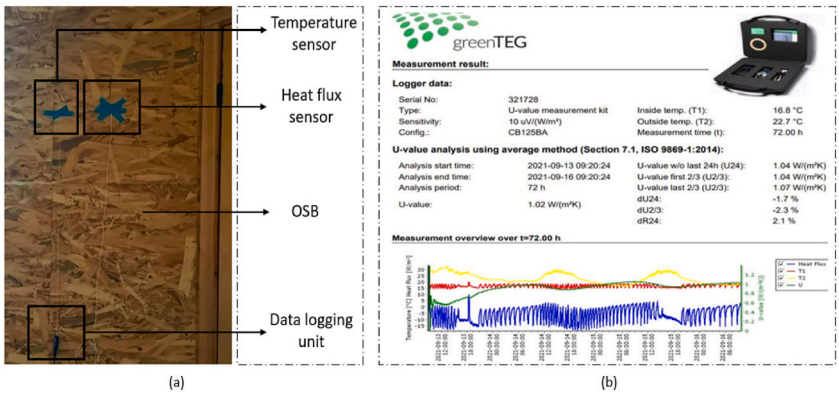

Fig. 6. Thermal transmittance measurement; (a) Experimental Setup, (b) Data logger measurement.

Moreover, using the HFM 446 Lambda device, the second test of thermal conductivity was conducted on all building construction layers. The thermal conductivity measurement using this device is based on many regulations including ASTM C518 [53], ISO 8301 [54], DIN EN 12664 [55], and DIN EN 12667 [56]. Three tests were undertaken for each of the construction materials including OSB wood, Polystyrene XPS insulation, and acrylic insulation as presented in Fig. 7.

2.2.2. Glass characterization measurement

The glazing is subject to degradation by many factors including extreme temperature and pressure fluctuations, exposure to Oxygen and Ozone as well and sunlight exposure [57]. Therefore, understanding the link between thermal performance and deterioration will help to enhance BEM and energy estimation, allowing the maximization of lifetime efficiency and more effectively managing retrofit needs. Thus, the SHGC was measured and compared with the manufacturer's values in this study to assess its condition and performance after the period of use (4 years). This evaluation aimed to determine whether the glazing had experienced any degradation over time. Therefore, the type of glass used in the building windows was detected using the Glass Check PRO model CG3001(Fig. 8). This device helps to detect the type of glazing either single, double, or triple-pane windows. It also helps in measuring the thickness of each layer including the space gap. Furthermore, the device allows the detection of the presence, the location, and the type of invisible Low-E coatings [58]. The measurement was applied to all the building windows and the glass doors.

Moreover, the optical properties of window glazing were detected using a Window Energy Profiler device model WP4500. This device helps with testing and measuring the ultraviolet transmission, near-infrared transmission, VLT, and the estimation of SHGC for transparent low-E or clear glazing [59,60]. The window energy profiler was used several times for all the building windows and glass doors, as shown in Fig. 9.

2.2.3. Blower door test – infiltration measurement

Infiltration is an important part of the building energy budget and was measured directly by the blower door test shown in Fig. 10. During this test, the VRF system was turned off and all its supply and exhaust grilles were closed. Then, a pressure of 50 Pa was fixed, rather than the volume of air changed under normal conditions. The results of the measured air change per hour under 50Pa were converted to normalized air change per hour using equation (1):

$$ACH_{Atmospheric} \approx \frac{ACH_{50}}{F} \tag{1}$$

Knowing that F factor relates the air change per hour under typical conditions ($ACH_{Atmospheric}$) to air change per hour under 50 Pa (ACH_{50}). The methodology of ACH calculation, developed by M. Royapoor et al. [61], was used in our study to calculate the normalized air change per hour.

2.3. Meteorological data measurement

The meteorological weather specifications, shown in Table 3, were extracted from a local weather station (Fig. 11) located on-site near the building in the Green Energy Park research platform. The resulting weather data were in EnergyPlus weather file format (.epw) with 1-min intervals. The data recorded from the weather station include air dry bulb temperature, air wet bulb temperature, atmospheric pressure, relative air humidity, dew point temperature, global solar irradiation, normal solar irradiation, diffuse solar irradiation, wind speed, and rainfall. Further and detailed information about the local weather station is described by Azouzoute et al. [62] and Abraim et al. [63].

2.4. Numerical model description

In this paper, the boundary conditions, including thermal zones and space types, along with the building geometry are defined using the OpenStudio 3.2.1 engine (compatible with EnergyPlus 9.5.0). The first step of the building energy model is the creation of the building geometry (Fig. 12) according to the building plans. The input parameters of the numerical base model were extracted from the building technical documentation. Table 4, presents the distribution of construction and insulation layers of each building component starting from the outer to the inner layer. Thermal conductivity, density, specific heat capacity as well and the theoretically calculated U-Value, were the thermal input parameters of the base model for the BEM along with glazing specifications presented in Table 5. The theoretical U-value of the opaque building construction materials was calculated according to ISO6946 [64] regulation taking into

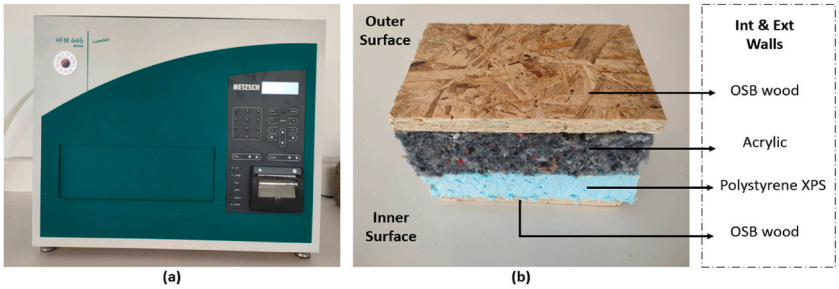

Fig. 7. Thermal conductivity measurement. (a): HFM 446 Lambda /(b): Wall composition.

Fig. 8. Glazing type measurement.

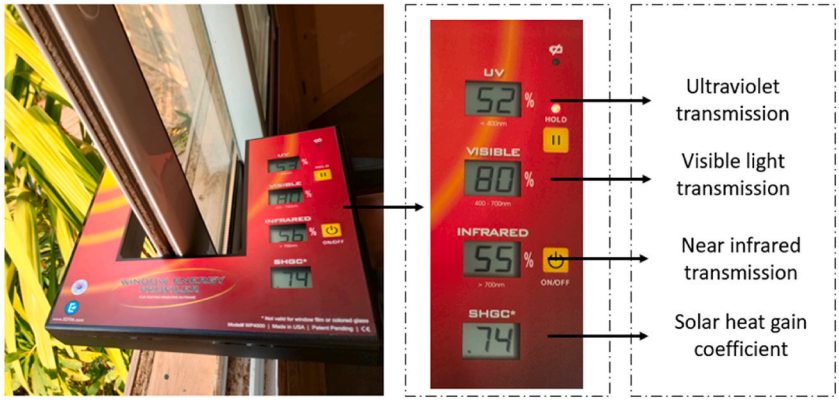

Fig. 9. Optical glazing properties measurement.

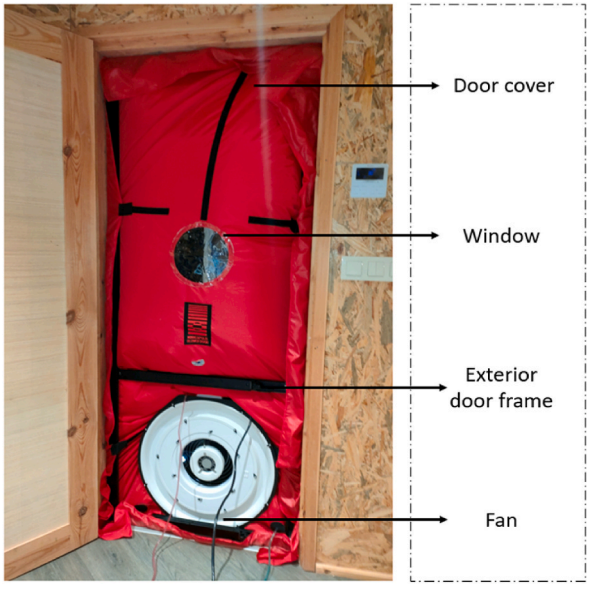

Fig. 10. Blower door test setup.

Table 3
Weather data.

Weather file	Ben Guerir Marrakech-Safi Morocco GEP_Station
Latitude	32.22
Longitude	−7.9
Elevation	475 m
Time zone	1.00
North Axis Angle	−45.0

Fig. 11. Local weather station.

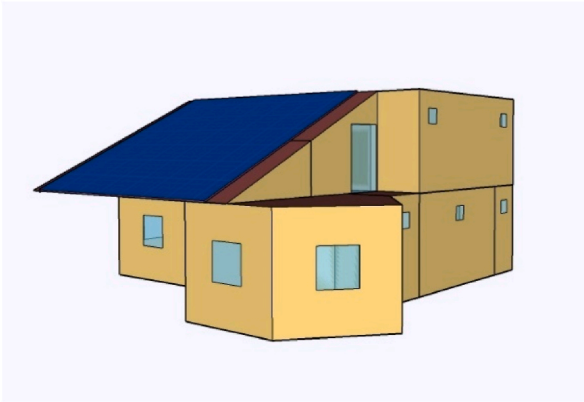

Fig. 12. OpenStudio 3D model of the case study building.

consideration the superficial resistances of the interior and the exterior according to horizontal and vertical walls. Besides, the infiltration level of the base model was set to 0.5 ACH as advised by the ASHRAE handbook [65]. Moreover, the external shading was considered as well in the developed BEMs. The building's north and south façades are exposed to nearby shadowing coming from trees and vegetation. Whereas, in the west and southwest building façade, there exists a neighboring building creating high shading for the building and especially for room 2. Moreover, the external shading in the east facades is neglected due to the distance between the building and the neighboring constructions which do not expose any shading in this facade.

Furthermore, the building is divided into 5 thermal zones served by a VRF system. For cooling and heating temperature setpoints, the used ranges are 24 °C–26 °C for cooling and 18 °C–20 °C for heating according to the Moroccan Thermal Regulation for Constructions [66]. Additionally, the VRF performance curves are crucial factors that must be taken into consideration during the creation of BEM. Since it depends on many factors including outdoor and indoor temperatures, outdoor unit total capacity, indoor unit total power input as well and refrigerant pipeline length corrections. As a result, using tabular data taken from the manufacturer's datasheet, 20 VRF performance curves were calculated [67,68]. The calculations have followed the methodology developed by Raustad et

Table 4
Input parameters of the building components.

Component	Layers (thickness)	Conductivity (W/m.K)	Density (kg/m^3)	Specific heat capacity (J/Kg.K)	Theoretical U – Value (W/m^2.K)
Roof	Waterproofing (15 mm)	0.0026	1042	880	0.28
	OSB 3 (15 mm)	0.13	600	1880	
	Polystyrene -XPS (40 mm)	0.034	32	1450	
	Acrylic (50 mm)	0.037	1390	1360	
	OSB 3 (15 mm)	0.13	600	1880	
Ceiling	Plywood (15 mm)	0.14	530	900	0.33
	Polystyrene -XPS (40 mm)	0.034	32	1450	
	Acrylic (50 mm)	0.037	1390	1360	
	OSB 3 (15 mm)	0.13	600	1880	
Ext & Int Walls	OSB 3 (15 mm)	0.13	600	1880	0,34
	Polystyrene -XPS (40 mm)	0.034	32	1450	
	Acrylic (50 mm)	0.037	1390	1360	
	OSB 3 (15 mm)	0.13	600	1880	
Ground floor	Polystyrene -XPS (40 mm)	0.034	32	1450	0,68
	Plywood (15 mm)	0.15	600	1600	

Table 5
Input parameters of the windows glazing building components.

Windows	Layers (Thickness)	Solar Heat Gain Coefficient (SHGC)	Visible transmittance light (VTL)	U- Value (W/m2.K)
Double Clear glazing	Clear glass (6 mm) Air gap (8 mm) Clear glass (6 mm)	0.70	0.78	2.89

all [69]. Table 6 summarizes all the performance curves of outdoor and indoor units along with their coefficients.

2.5. Numerical model improvement process & evaluation

The main aim of this research is to create an easy, feasible, and precise strategy for evidence-based building energy model validations, that can be used by researchers as a basis by providing enormous data for building validation using lightweight building constructions with the use of VRF systems, especially in the semi-arid climate. This methodology takes the advantage of using accurate input data for the BEM which were extracted using experimental setups. Fig. 13, shows the detailed methodology used for the improvement of the numerical base model. Starting with a base model created from the building's as-built drawings and technical reports. The thermal characteristics of opaque and glazing materials were extracted from the manufacturer datasheets, and calculated theoretically. The infiltration was set to 0.5 ACH based on ASHRAE55 recommendations. Then, the statistical indices were calculated for the hourly measured and simulated VRF energy consumption and indoor temperatures. Three other improved BEMs have been conducted based on several experimental measurements for the enhancement of the building numerical model.

In model 1, the building envelope thermal transmittance was estimated based on the thermal conductivity test measurements conducted using HFM 446 Lambda. All the other parameters of the base model were conserved in model 1. Model 2 is the third simulation conducted after the in-situ investigation of the glazing thermal properties. The extracted layers of the existing windows and their thickness were set as input in model 2, as well as the real measured SHGC and VLT values. In Model 3, the building airtightness obtained from the in-situ infiltration measurement was set as input to model 3 along with all the other input parameters of Model 2. The numerical model validation was conducted on hourly energy consumption for cooling and heating periods along with the hourly indoor temperature on a nearly complete year of dataset starting from the 22nd of January 2021 until the 31st of December 2021. The measured temperature data of room 1 were missing from the 1st of January until the 21st of January and from the 22nd of October until the 10th of November. Besides, in room 2, data was missing for the whole month of January and from June until the end of the year. This was due to several technical problems that occurred in the data acquisition system.

The statistical indices used in this study are CV(RMSE) and NMBE. The CV(RMSE) is calculated mathematically using equation (2), to model the difference in uncertainty between the simulated and measured data;

$$CVRMSE = 100 \left[\frac{\sum_{i=1}^{n} (y_i - \hat{y}_i)^2}{n} \right]^{1/2} \Big/ \bar{y} \tag{2}$$

Knowing that y is real data, $\hat{y}$ is simulated data, $\bar{y}$ is the mean of measured data and n corresponds to the overall sum of hours

Table 6
List of VRF performance curves calculated parameters values.

	Coefficient 1	Coefficient 2	Coefficient 3	Coefficient 4	Coefficient 5	Coefficient 6
OUTDOOR UNIT						
Cooling capacity ratio modifier function of low-temperature curve	−3.233217934	0.409109691	−0.00892928	−0.001508216	1.08994e-05	6.84153e-05
Cooling capacity ratio boundary curve	−427.7806956	74.49094499	−3.775720705	0.059606481	–	–
Cooling capacity ratio modifier function of high-temperature curve	−2.747086658	0.253518571	−0.003771626	0.067504335	−0.000736983	−0.001493169
Cooling energy input ratio modifier function of low temperature	−1.65079921	0.209854131	−0.004740193	−0.025614299	0.000438904	–
Cooling energy input ratio boundary curve	−427.7806956	74.49094499	−3.775720705	0.059606481	–	–
Cooling energy input ratio modifier function of high-temperature curve	−7.736056351	0.577354048	−0.009995146	0.123947432	−0.000439784	−0.003252722
Cooling energy input ratio modifier function of low-part load ratio curve	0.026031746	0.520829852	0.355889724	0.097465887	–	–
Cooling combination ratio correction factor curve	0.83317757	0.171728972	–	–	–	–
Piping correction factor for length in cooling mode	1.010089286	−0.001261905	1.4881e-06	–	–	–
Heating capacity ratio modifier function of low-temperature curve	1.076797127	−0.00977627	0.000222036	0.025968534	0.000449937	−5.03891e-06
Heating capacity ratio boundary curve	148.2376118	−21.55668359	1.099226493	−0.019458545	–	–
Heating capacity ratio modifier function of high-temperature curve	1.605559687	−0.030264728	−1.37054e-05	0.001319945	−1.57385e-05	−3.59442e-05
Heating energy input ratio modifier function of low-temperature	1.0674324	−0.002203648	0.000246162	0.021452477	1.56847e-05	−0.000573529
Heating energy input ratio boundary curve	148.2376118	−21.55668359	1.099226493	−0.019458545	–	–
Heating energy input ratio modifier function of high-temperature curve	1.944294572	−0.031118413	−0.000390442	−0.060657897	0.000661649	0.00117028
Heating energy input ratio modifier function of low-part load ratio curve	0.012093726	0.866244646	0.011337868	0.110229277	–	–
Heating combination ratio correction factor curve	0.705975644	0.328518833	–	–	–	–

(*continued on next page*)

Table 6 (*continued*)

	Coefficient 1	Coefficient 2	Coefficient 3	Coefficient 4	Coefficient 5	Coefficient 6
Piping correction factor for length in heating mode	0.983153557	0.001821543	−1.36358e-05	–	–	–
INDOOR UNIT						
Cooling capacity ratio modifier function of temperature curve	−1.0671939	0.134774478	−0.001333867	0.016084039	−4.3846e-05	−0.000829064
Heating capacity ratio modifier function of temperature curve	0.915061054	0.008566716	−0.000514892	0.035709143	−0.000251964	−0.001167757

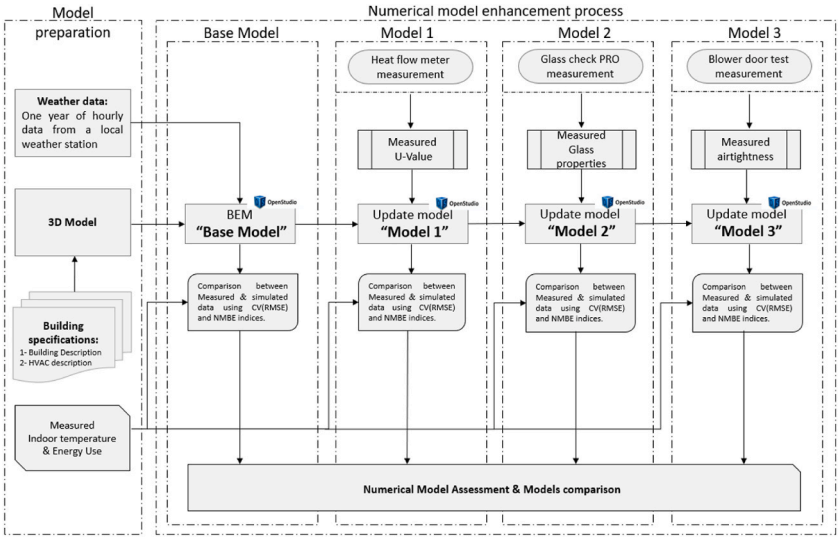

Fig. 13. Numerical model improvement process.

depending on the time frame used (week, month, year). The second statistical indices used in this study is the NMBE, which is calculated using equation (3):

$$NMBE = \frac{\sum_{i=1}^{n}\left(y_i - \hat{y}_i\right)}{n \times \bar{y}} * 100 \tag{3}$$

After the improvement and validation of the BEMs, the accurate model was selected for further evaluation of the building energy use in all the Moroccan regions and climatic zones selected according to the Moroccan Thermal Regulation for Constructions [66]. A standard office occupancy schedule was used for this evaluation. This evaluation aims to assess the impact of implementing this lightweight structure with the VRF system in all Moroccan regions, to evaluate the building energy efficiency regarding these different climates.

3. Results and discussion

3.1. Evidence-based data acquisition

To collect evidence-based data, several in-situ measurements were conducted to extract the crucial building parameters that affect the BEM accuracy based on the conducted sensitivity analysis. Thus, Table 7, summarizes the results of the measured thermal transmittance using the GreenTEg device along with the deviation between theoretical and measured U-value of the building's external walls. According to these findings, the deviation between all the conducted in-situ measurements is representative.

Table 7
Measured thermal transmittance using GreenTeg vs. theoretical transmittance data.

	Thermal transmittance (W/m^2K)					
	Measurement 1	Measurement 2	Measurement 3	Average	Theoretical	Deviation
External walls	1.02	0.74	0.78	0.84	0.34	0.50

Table 8
Measured thermal conductivity using HFM 446 Lambda Vs known conductivity data.

Materials	Thermal conductivity (W/mK)					
	M 1	M 2	M 3	Average	Manufacturer	Deviation
OSB wood	0.108	0.105	0.104	0.106	0.130	−0.024
Polystyrene	0.042	0.040	0.039	0.040	0.034	0.006
Acrylic	0.044	0.042	0.042	0.042	0.037	0.005

Table 9
Comparison between glazing manufacturer data and measured ones.

	Manufacturer data	Measured data
Double glazing (Layers, thicknesses)	Clear glass (6 mm) Air gap (8 mm) Clear glass (6 mm)	Clear glass (5.5 mm) Air gap (7.6 mm) Clear glass (5.5 mm)
SHGC	0.70	0.74
VLT	0.78	0.80

Since the great variation between measured and theoretically calculated U-value, a second series of measurement tests was conducted for the thermal conductivity of construction and insulation materials, using this time the HFM 446 Lambda, to make sure of the measured U-value accuracy. The results of the thermal conductivity tests on each material are shown along with their deviation from known conductivity data, in Table 8. Therefore, the deviation between measured and known values of thermal conductivity is not representative. Thus, according to both experimental tests, the first U-value measurements obtained with the GreenTeg logger are not accurate and widely different from the theoretical values. Despite the consideration of many parameters during the conduction of the test measurements, the obtained results are not reliable. Moreover, the second measurement conducted using the HFM 446 Lambda gives accurate results similar to the theoretical and known thermal conductivity values. So, for the rest of this study, theoretical values of the U-value were used for the generation of the first base model. Then, the measured values obtained using the HFM 446 lambda were used for the generation of model 1.

The second evidence-based measurement was applied to the building glazing to extract the thermal and optical properties of glazing windows. The findings of each measurement were the same in the majority of the building's windows. Table 9 presents the manufacturer's glazing data along with measured glazing specifications. According to these findings, there is only a slight difference regarding real thicknesses of the glazing layers as well as the values of SHGC and VLT. Therefore, these real measured glazing parameters were used for the improvement of the BEM in model 2.

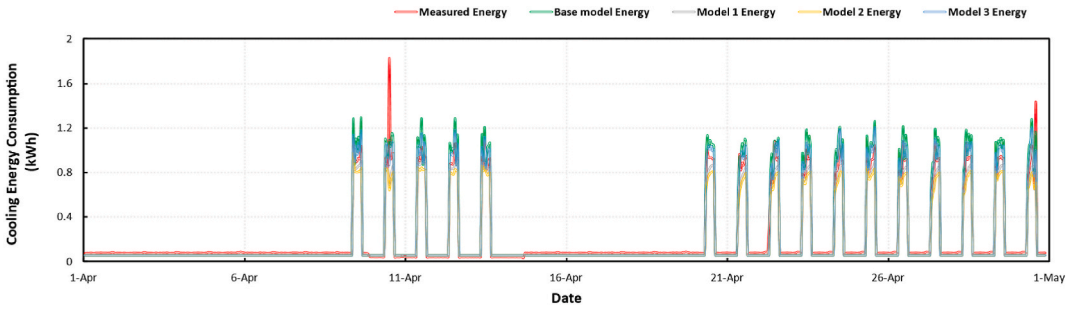

Fig. 14. Measured and simulated hourly energy consumption in cooling period.

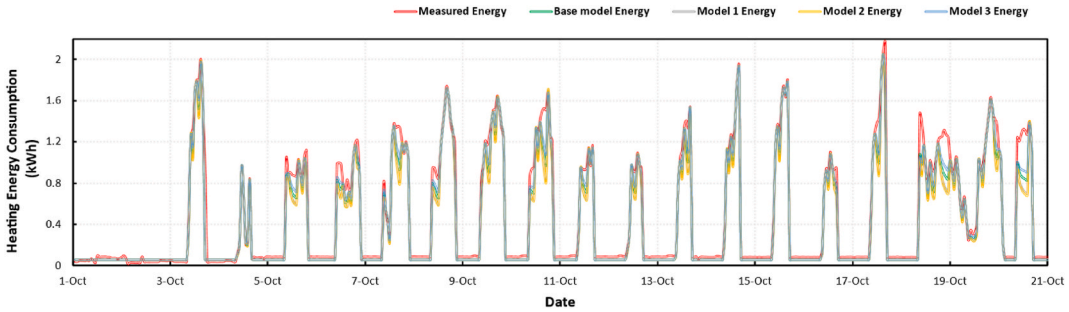

Fig. 15. Measured and simulated hourly energy consumption in heating period.

Table 10
Monthly NMBE and CV(RMSE) for hourly VRF energy consumption.

Months	Base Model		Model 1		Model 2		Model 3	
	CV(RMSE) [%]	NMBE [%]	CV(RMSE) [%]	NMBE [%]	CV(RMSE) [%]	NMBE [%]	CV(RMSE) [%]	NMBE [%]
April	38.78	−16.04	33.52	−14.11	33.30	−12.8	28.49	−6.12
October	31.17	14.37	24.81	11.77	30.07	13.91	20.57	9.77

Moreover, the building airtightness measurement was conducted using the blower door test. The found infiltration level was 1.5 ACH, this value will be used for the enhancement of the numerical model in model 3.

3.2. Energy evaluation

The results of simulated and measured hourly VRF energy consumption in cooling and heating periods are shown respectively in Figs. 14 and 15, for each model. Table 10, presents the variation of CV(RMSE) and NMBE for hourly VRF energy use of the four models.

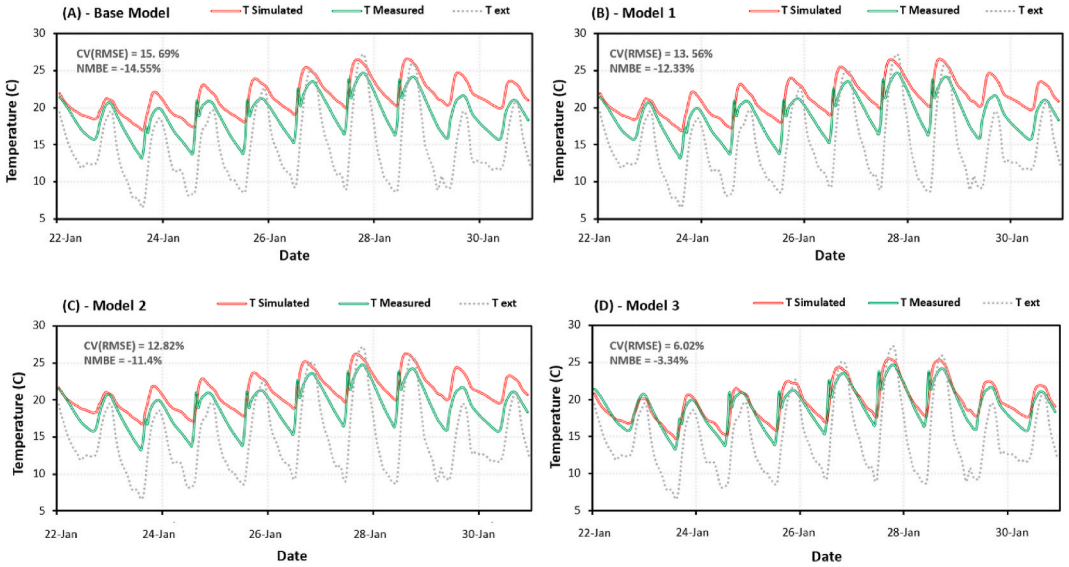

Fig. 16. Daily measured and simulated hourly temperature data in winter season for room 1.

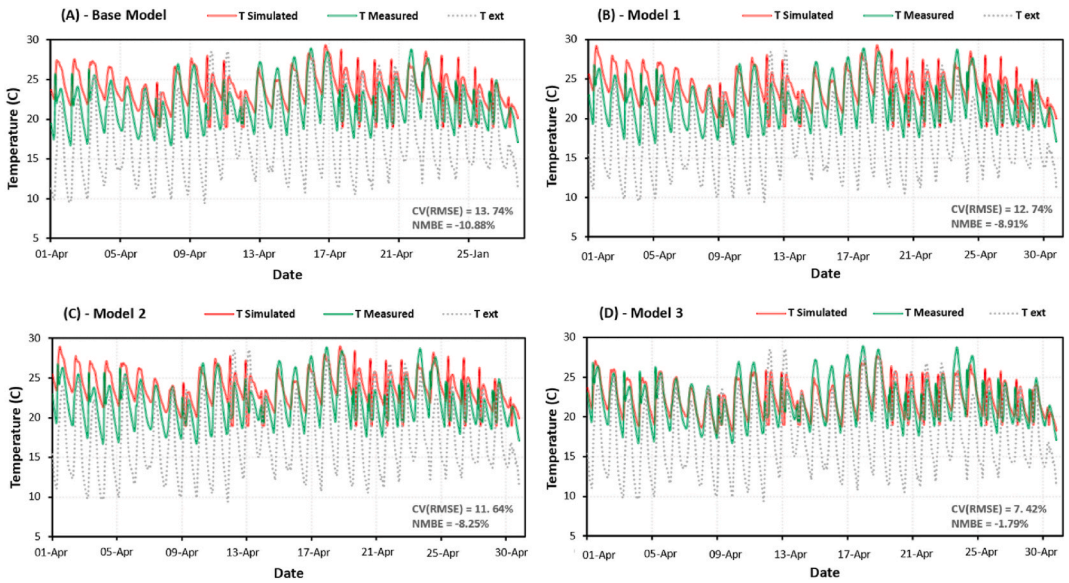

Fig. 17. Daily measured and simulated hourly temperature data in spring season for room 1.

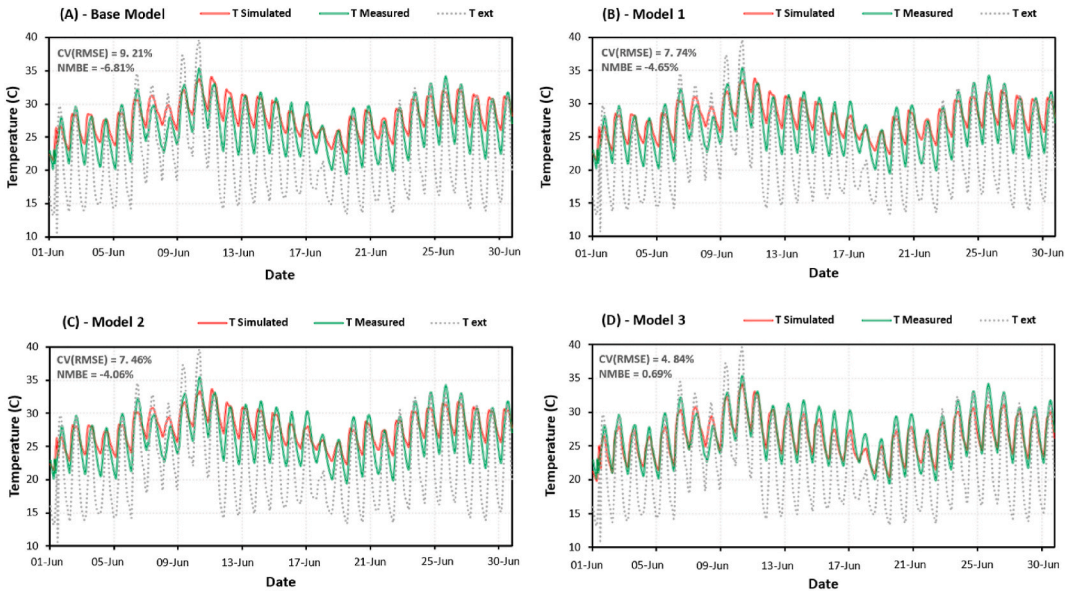

Fig. 18. Daily measured and simulated hourly temperature data in summer season for room 1.

The findings of the VRF energy consumption assessment, prove the invalidation of the BEM either in the cooling period of April or in the heating period of October for the base model, model 1, and model 2, unlike model 3 which is validated for both periods. Therefore, the energy use data has improved through the enhancement of the numerical model using evidence-based measured data. Moreover, the cooling and heating energy consumption is impacted by the indoor temperature and the HVAC system type using performance curves as well as the weather conditions. Besides, the indoor temperature is highly impacted by the construction materials' thermal conductivity, the glazing thermal and optical parameters as well as the building infiltration. Therefore, the developed model has a high accuracy since all these parameters were measured locally to make sure from the real values of the building simulation parameters and the numerical model precision.

3.3. *Indoor temperature evaluation*

The results of indoor temperature validation in room 1 are presented in Fig. 16 for winter season, in Fig. 17 for spring season, in Fig. 18 for summer season, and in Fig. 19 for autumn season along with statistical indices of each model. In the base model, the findings of the predicted indoor temperature show a difference regarding the measured indoor temperature. Moreover, the calculation of the

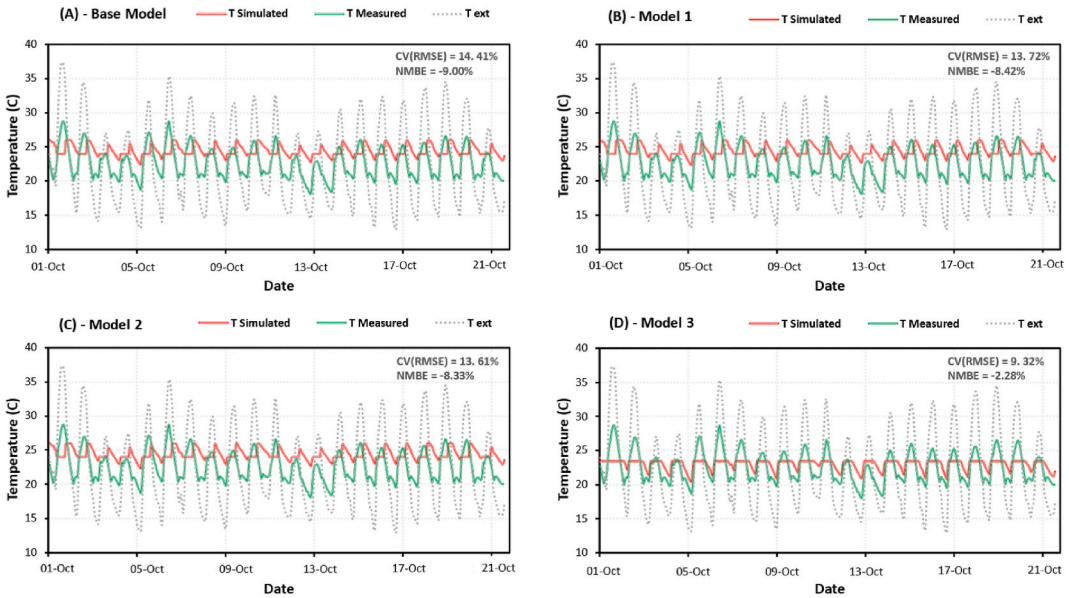

Fig. 19. Daily measured and simulated hourly temperature data in autumn season for room 1.

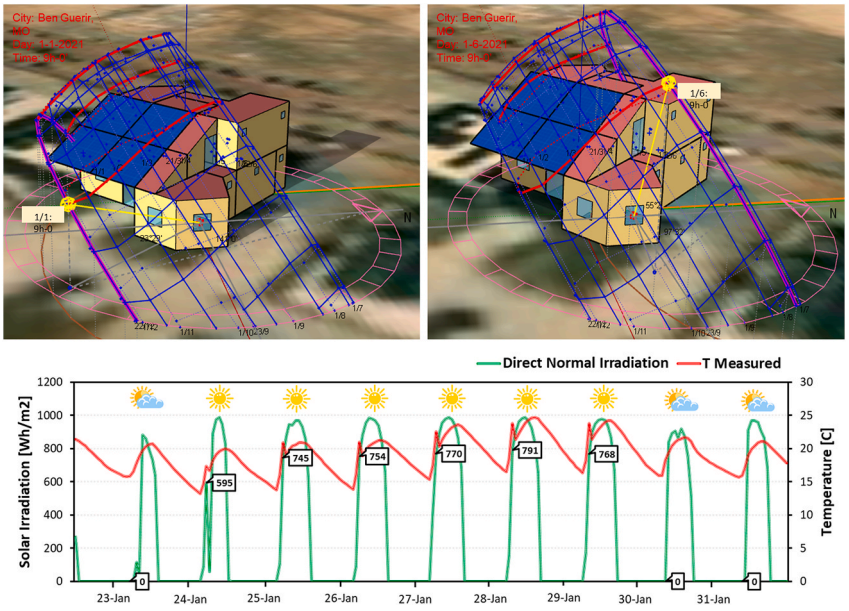

Fig. 20. Peak direct solar irradiation occurrence time. (a) On the first day of January at 09 a.m. (b) On the first day of June at 09 a.m. (c) During 2 weeks in January.

statistical indices proves that the input data of the model do not follow real data. This could be explained by the flawed assumptions made based on the literature which did not line up with the building's actual existent specifications. Therefore, to improve the results of the base model a second simulation, Model 1, has been carried out. The hourly indoor temperature results show a slight difference compared with the base model**.** Whereas, the findings of model 2 show an improvement compared with the base model and model 1. However, model 3 provides the best results of indoor temperature matching with measured data.

Based on the graphs of the daily measured and predicted indoor temperature for winter season presented in Fig. 16, the existence of a temperature peak in the measured indoor temperature can be noticed. This peak is due to the poor location of temperature sensor, which is near an existing window. Based on Fig. 20, the temperature peak happens at 09 a.m. In January, the sun trajectory is in front of the window of room 1 in the mornings. Thus, each sunny morning at 09 a.m. the solar radiations are projected directly on the temperature sensor inside room 1. Otherwise, in June the trajectory of the sun is higher and far from the room's window. Thus, in June as presented in Fig. 18, there is no peak in indoor temperature and the measured indoor temperature is the same as the simulated indoor temperature for model 3.

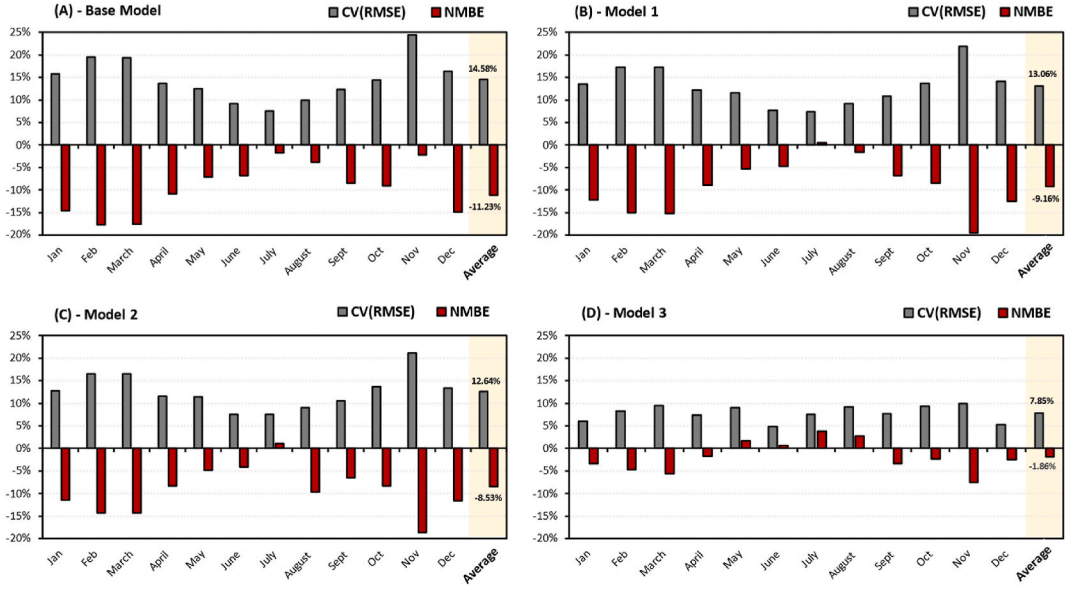

Fig. 21. Annual average CV(RMSE) and NMBE in room 1.

Table 11
Monthly NMBE and CV(RMSE) values for the hourly indoor temperature of room 1.

Months	Base Model		Model 1		Model 2		Model 3	
	CV(RMSE) [%]	NMBE [%]	CV(RMSE) [%]	NMBE [%]	CV(RMSE) [%]	NMBE [%]	CV(RMSE) [%]	NMBE [%]
January	15.69	−14.55	13.56	−12.23	12.82	−11.40	6.09	−3.34
February	19.56	−17.70	17.20	−15.11	16.47	−14.26	8.35	−4.72
March	19.41	−17.59	17.27	−15.22	16.52	−14.34	9.44	−5.61
April	13.74	−10.88	12.14	−8.91	11.64	−8.25	7.42	−1.79
May	12.51	−7.05	11.60	−5.38	11.34	−4.83	9.06	1.67
June	9.21	−6.81	7.74	−4.65	7.46	−4.06	4.84	0.69
July	7.60	−1.69	7.38	0.48	7.49	1.02	7.57	3.86
August	9.87	−3.82	9.12	−1.54	9.09	−0.96	9.12	2.71
September	12.26	−8.45	10.86	−6.89	10.57	−6.52	7.69	−3.42
October	14.41	−9.00	13.72	−8.42	13.61	−8.33	9.32	−2.28
November	24.37	−22.26	21.95	−19.54	21.20	−18.71	9.92	−7.57
December	16.31	−14.93	14.11	−12.43	13.42	−11.64	5.31	−2.53
Average	14.58 %	−11.23 %	13.06 %	−9.16 %	12.64 %	−8.53 %	7.85 %	1.86 %

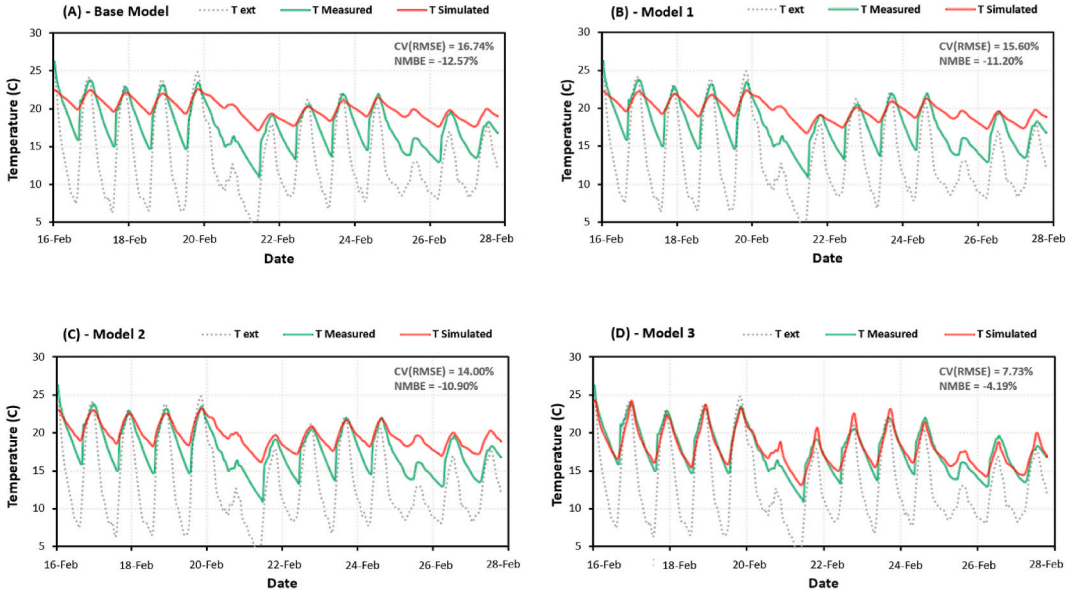

Fig. 22. Daily measured and simulated hourly temperature data in winter season for room 2.

Furthermore, in model 3 presented in Fig. 17, there exist some gaps between measured and simulated indoor temperature. These gaps are due to the building openings for cleaning and equipment maintenance. These openings were not taken into consideration in simulation, as a result, these little changes in input data have led to small temperature fluctuations. Otherwise, the slight difference between measured and simulated indoor temperature presented in Fig. 19, is related to the occupants' behavior. As of October, the VRF system was working in heating mode. Whereas, the developed BEM for the aim of this study, the thermal comfort heating and cooling setpoints recommended by the Moroccan Thermal Regulation for Constructions were used as HVAC temperature setpoints. Nevertheless, in reality, the occupants used to operate the heating thermostat differently.

Moreover, as shown in Fig. 21, the base model has an annual average CV(RMSE) of 14.58 %, hence model 1 has a value of 13.06 %. Regarding the NMBE, the base model represents an annual average value of −11.23 %, and model 1 has an annual average value of −9.16 %. Therefore, the thermal transmittance of the building envelope is not enough to improve the accuracy of the model. Thus, this proves that the thermal characteristics of the construction and insulation materials taken from the manufacturer's datasheets were approximately accurate with a small difference caused by material ages. This difference, as explained previously, is due to the degradation of the envelope materials. However, the findings of model 1 have slightly improved according to the base model. Still, model 1 is not validated for the whole year and should be more improved. Therefore, in model 2 the annual average of the CV(RMSE) and the NMBE are respectively 12.64 % and −8,53 %. Additionally, the results of all months have improved compared to the base model and model 1, although there still are months that have not been validated yet. Thus, the building glazing parameters highly impact the fluctuation of the indoor temperature. So, before starting a building calibration process, it is crucial to make sure of the input glazing parameters. Furthermore, the results of model 3, show the model validation for the whole year, and its accuracy regarding model 2. Based on this finding, it's concluded that infiltration is also an important parameter that should be taken into consideration while conducting a numerical BEM. The range of infiltration given in literature is between 0.5-1ACH and the most used

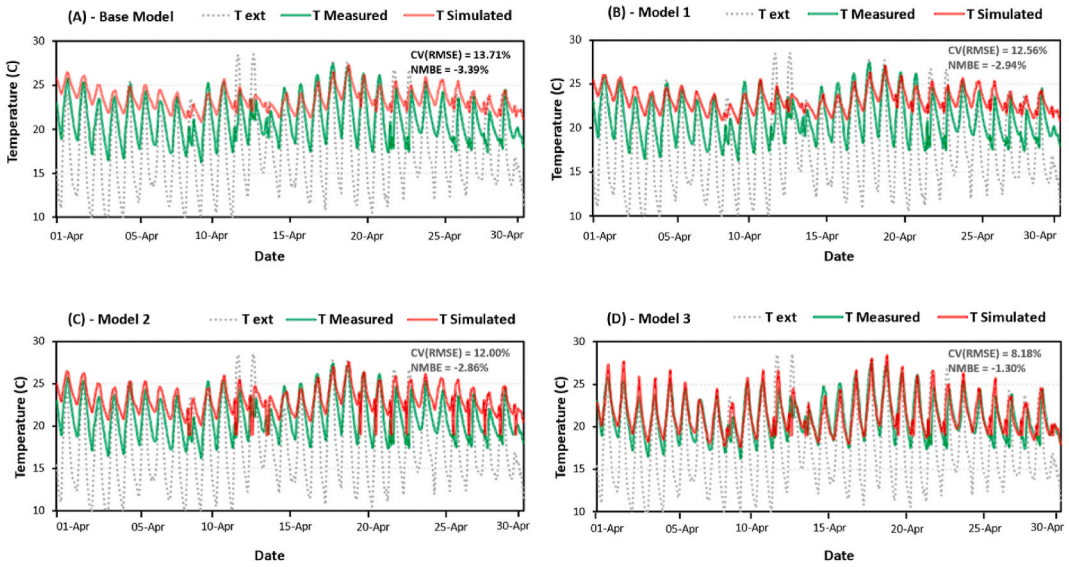

Fig. 23. Daily measured and simulated hourly temperature data in spring season for room 2.

Table 12
Monthly NMBE and CV(RMSE) for hourly indoor temperature of room 2.

Months	Base Model		Model 1		Model 2		Model 3	
	CV(RMSE) [%]	NMBE [%]	CV(RMSE) [%]	NMBE [%]	CV(RMSE) [%]	NMBE [%]	CV(RMSE) [%]	NMBE [%]
February	16.74	−12.57	15.60	−11.20	14.00	−10.98	7.73	−4.19
March	16.85	−13.80	15.70	−12.55	14.91	−12.76	9.29	−6.93
April	13.71	−3.39	12.56	−2.94	12.00	−2.86	8.18	−1.30
May	16.87	−6.44	15.56	−5.79	15.87	−5.79	12.99	−2.88
Average	12.04	−9.05	14.85	−8.12	14.19	−8.09	9.54	−3.82

value is 0.5ACH. So, based on this assumption we used 0.5 ACH as the base model input infiltration. Nevertheless, this value could not always be accurate for all building constructions. In our case, the building is built from wood with an insufficient insulation layer, the infiltration found using the blower door test is 1.5ACH. Thus, according to the results of model 3, we could notice that all the months are calibrated and respect the acceptable tolerances. So, this finding proved the accuracy of the BEM developed in the aim of this study, and all the input parameters of the simulation are approximately the same as the real ones over time and seasons. This study has shown that there is a good agreement between the measured and simulated hourly energy consumption and indoor air temperatures.

Both statistical indices values for each month for all models are presented in Table 11. The comparison of indoor temperature predictions against experimental ones of room 1 of all models proves that BEM could be validated in some periods of the year but not validated for all the year, which is the case for the base model, models 1 & 2, unlike model 3 that was validated for the whole year. Therefore, it is crucial to conduct a validation strategy for the whole year.

According to the aforementioned findings, the BEM of the whole building with several thermal zones was validated against a unique temperature measurement in room 1. Therefore, to verify the accuracy of the developed model 3, the results of the hourly indoor temperature in a second thermal zone (room 2) are assessed. These two rooms have completely different conditions, and if both of them are validated using model 3, it could be concluded that the whole building is validated. The measured hourly temperature of room 2 was only recorded from February until May. These measured data were compared to the simulated ones using the four developed models. Fig. 22 & Fig. 23 present respectively the variation of the measured and simulated indoor temperature inside room 2 for all models. Table 12, shows that room 2 is also validated using model 3 with an average of 9.54 % for CV(RMSE) and −3.82 % for NMBE.

3.4. Energy evaluation in Morocco

After the enhancement of the base energy model with several in-situ measurements, the final precise model, model 3, was used as reference in 12 Moroccan regions. Fig. 24, summarizes the cooling energy consumption of lightweight construction in Morocco. The region of Guelmim-Oued Noun has the lowest cooling energy, unlike the region of Deraa-Tafillalet which has the highest cooling energy consumption compared to all the other regions. Therefore, this lightweight building structure could be beneficial for Guelmim-Oued Noun in cooling periods.

The variation of the heating energy use in Moroccan regions is represented in Fig. 25. The Dakhla-Oued Ed-Dahab region has the lowest heating energy use, while the Fes-Meknes region has the highest heating energy consumption. Therefore, the southern regions

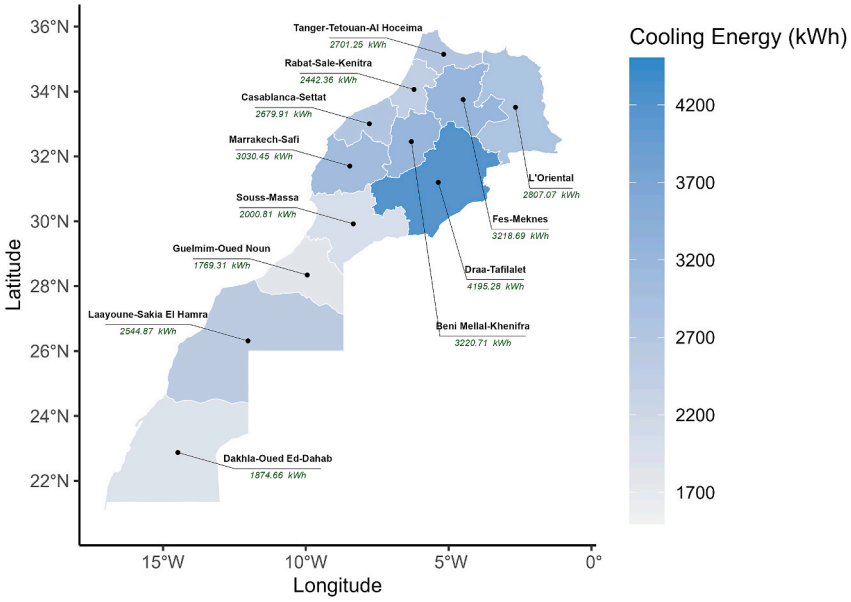

Fig. 24. Cooling energy evaluation in Morocco.

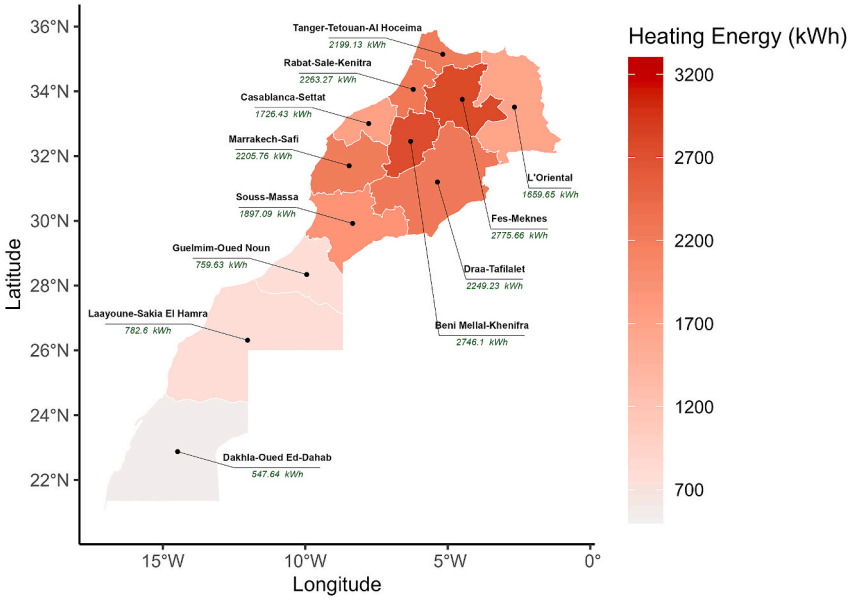

Fig. 25. Heating energy evaluation in Morocco.

are best locations to use such buildings with a VRF system.

The six climatic regions of Morocco are presented in Table 13 along with their cooling and heating energy use. Ifrane region has the lowest cooling energy and also the highest heating energy use. Therefore, this building construction would not be sufficient in cold seasons in Ifrane zone, unlike Agadir zone which has the lowest heating energy and also second lowest cooling energy.

4. Potential building improvement in Morocco

The energy policy for the building sector in Morocco is distinguished by a strong commitment to energy efficiency and sustainability. The country is conscious of the importance of the building sector as a significant energy consumer and source of greenhouse gas emissions. To address these challenges, Morocco has implemented several key initiatives:

Table 13
Energy evaluation according to Moroccan climatic zones.

Climatic Zones	Cooling Energy (kwh)	Heating Energy (kwh)
Agadir	2000.81	1897.09
Tanger	2701.25	2199.13
Fes	3218.69	2775.66
Ifrane	1532.81	3800.45
Marrakech	3030.45	2205.76
Errachidia	4195.28	2249.23

Table 14
Highlight of some studies that contribute in the improvement of buildings thermal performance for the Moroccan context.

Reference	Contributions in enhancing buildings performance for Moroccan context
Romani et al. [73]	The authors have conducted a building envelope optimization to decrease the overall annual building energy loads in all the climates zones of Morocco
Hamdaoui et al. [74]	The authors have evaluated three Moroccan construction scenarios for an office building under the six climate zones of Morocco. Several passive energy efficient strategies were examined for the decrease of the annual energy demand and the greenhouse gases emissions.
Abdou et al. [75]	The authors have conducted a multi-objective optimization using passive energy efficient designs for the minimization of the building life-cycle cost as well as increasing both the energy savings and the indoor thermal comfort in all the Moroccan climatic zones.
Benallel et al. [76]	The authors have conducted a thickness optimization of exterior wall insulation for different climatic regions in Morocco for the determination of the optimal insulation thicknesses, energy savings and payback periods.

- Building Codes and Standards: To enhance the energy efficiency of both new and existing buildings, Morocco has implemented strict building regulations and standards. The aforementioned regulations mandate energy-efficient HVAC systems, energy-efficient insulation, and energy-efficient lighting [66].
- Renewable Energy Integration: The country promotes the incorporation of renewable energy sources into building designs. Buildings are increasingly powered by solar panels and other alternative energies, which lowers their dependency on conventional energy sources [70].
- Financial Incentives: To encourage the use of energy-efficient building techniques, Morocco provides financial incentives and subsidies. Tax breaks down, grants, and low-interest loans are among the incentives offered to encourage property owners and developers to invest in energy-efficient technologies [71].
- Green Building Certification: Green building initiatives that satisfy particular sustainability standards are promoted and certified by the Moroccan Green Building Council. This certification approach encourages architects, engineers, and developers to use environmentally friendly materials and practices [72].

By concentrating on these techniques, Morocco intends to decrease building sector energy consumption, lower greenhouse gas emissions, and improve the overall sustainability of its built environment. This is in line with the country's wider objectives of shifting to a greener and more energy-efficient economy while addressing concerns about climate change. Therefore, the findings of this proposed study are aligned with the energy policy and practices in Morocco. Since, the cooling and heating energy consumed with actual studied building respects and meets the thermal regulations of construction requirements in Morocco. Moreover, the literature show a diversity of studies that have focused on investigating the building cooling and heating energy uses in the six climatic zones of Morocco following the Moroccan energy codes and policies. Table 14 highlights some important studies that have contributed in the improvement of buildings thermal performance for the Moroccan context.

Hence, all the aforementioned studies have reached significant savings and improvement using different passive design strategies. Still, none of them have investigated and taken into consideration the lightweight construction envelope. Therefore, the present study could be of high interest and implications for similar climates and also for other building typologies. Moreover, the lightweight construction building envelope still needs more advanced enhancement techniques to be more energy efficient. Thus, Liu [77] have proved that the integration of phase change materials (PCM) could enhance the thermal performance of lightweight building constructions using the suitable phase-transition temperature, optimal locations of PCM in different orientations of the construction resulting in significant thermal performance improvement. This promotes the integration of innovative and new materials to the building construction, which may have the potential to improve the built environment.

5. Conclusions and future work

In this paper, a thorough investigation into improving a numerical Building Energy Model (BEM) for an existing lightweight building with a Variable Refrigerant Flow (VRF) system in a semi-arid climate was conducted. Using the OpenStudio simulation engine with a 1-min timestep, we aimed to enhance the accuracy of the BEM by integrating real-world building parameters obtained through on-site measurements. The key findings of the proposed study are as follows:

1. Temporal Scale for Enhancement: Enhancing the numerical model should be carried out on an annual basis. It was found that some months within a year may not align well with real-world conditions due to variations in input parameters. Ensuring the model's applicability for the entire year is crucial, especially for applications such as energy consumption forecasting.

2. HVAC Energy Validation: It's essential to validate HVAC energy consumption during both cooling and heating seasons. Relying solely on indoor temperature validation may not guarantee the accuracy of the entire building's energy systems, as these systems are influenced by performance curves, indoor temperature, and weather conditions. Therefore, it's vital to validate energy consumption alongside indoor temperature.
3. In-Situ Measurements Importance: Before developing any numerical BEM, conducting comprehensive in-situ measurements of the building's characteristics and equipment is paramount. Accurate calibration of the model depends on input parameters closely matching their real-world counterparts, with special attention to parameters like the building infiltration rate.
4. Energy Efficiency of Lightweight Buildings with VRF: this study suggests that using lightweight building construction combined with a VRF system can yield energy efficiency benefits, particularly in regions with high cooling and heating energy savings potential, such as Southern areas and Sub-Saharan regions.

In summary, this research underscores the significance of meticulous modeling and validation processes for BEMs to accurately assess building performance and energy efficiency, especially in varying climatic conditions. Moreover, future research should emphasize comprehensive sensor deployment, accurate BEM calibration, strategic sensor placement, and the adoption of energy-efficient building technologies to advance our understanding of building performance and promote energy efficiency across various regions.

Credit author statement

Niima Es-sakali: Conceptualization, Methodology, Investigation, Software, Formal analysis, Data curation, Writing - Original Draft, Visualization., Samir Idrissi Kaitouni: Methodology, Investigation, Software, Writing - Review & Editing., Imad Ait Laasri: Investigation, Formal analysis, Data curation, Writing - Original Draft, Visualization., Mohamed Oualid Mghazli: Investigation, Resources, Project administration, Writing - Review & Editing., Moha Cherkaoui: Writing - Review & Editing, Resources, Supervision., Moritz Bühler: Writing - Review & Editing., Jens Pfafferott: Writing - Review & Editing, Resources, Supervision, Funding acquisition.

Declaration of competing interest

The authors declare that they have no known competing financial interests or personal relationships that could have appeared to influence the work reported in this paper.

Data availability

Data will be made available on request.

Acknowledgment

This work was conducted in the Green & Smart Building Park – GSBP of the Green Energy Park platform (IRESEN, UM6P) and in collaboration with the Institute of Sustainable Energy Systems at Offenburg University of Applied Sciences. The building studied in this paper was built within the framework of the Solar Decathlon Africa competition. The authors of this paper would like to thank the DAAD (German Academic Exchange Service) for the funding of this work through the "Village.School" project.

References

[1] M. Cellura, F. Guarino, S. Longo, M. Mistretta, A. Orioli, The role of the building sector for reducing energy consumption and greenhouse gases: an Italian case study, Renew. Energy 60 (2013) 586–597.
[2] C. Shen, J. Peng, D. Wang, G. Pei, Recent advances in multispectral solar energy technologies for the building sector, Renew. Energy (2022). Elsevier.
[3] E. I. A. (US), Annual Energy Outlook 2012: with Projections to 2035, Government Printing Office, 2012.
[4] Z. Wang, Y. Wang, R.S. Srinivasan, A novel ensemble learning approach to support building energy use prediction, Energy Build. 159 (2018) 109–122.
[5] R.Ž. Jovanović, A.A. Sretenović, B.D. Živković, Ensemble of various neural networks for prediction of heating energy consumption, Energy Build. 94 (2015) 189–199.
[6] Z. Yu, F. Haghighat, B.C.M. Fung, H. Yoshino, A decision tree method for building energy demand modeling, Energy Build. 42 (10) (2010) 1637–1646.
[7] Y. Ma, F. Borrelli, Fast stochastic predictive control for building temperature regulation, in: 2012 American Control Conference (ACC), 2012, pp. 3075–3080.
[8] S. Huang, Y. Lin, V. Chinde, X. Ma, J. Lian, Simulation-based performance evaluation of model predictive control for building energy systems, Appl. Energy 281 (2021), 116027.
[9] L. Zhang, C. Hou, J. Hou, D. Wei, Y. Hou, Optimization analysis of thermal insulation layer attributes of building envelope exterior wall based on DeST and life cycle economic evaluation, Case Stud. Therm. Eng. 14 (2019), 100410.
[10] I. Ait Laasri, A. Outzourhit, M.O. Mghazli, Multi-parameter analysis of different building forms in a semi-arid climate: effect of building construction and phase change materials, Sol. Energy 250 (2023) 220–240.
[11] I. Ait Laasri, N. Es-sakali, A. Outzourhit, M.O. Mghazli, Numerical building energy simulation with phase change materials including hysteresis effect for different square building cases in a semi-arid climate, in: 2022 13th International Renewable Energy Congress (IREC), 2022, pp. 1–4, https://doi.org/10.1109/IREC56325.2022.10002008.
[12] N. Cauchi, K. Macek, A. Abate, Model-based predictive maintenance in building automation systems with user discomfort, Energy 138 (2017) 306–315.
[13] N. Es-sakali, M. Cherkaoui, M.O. Mghazli, Z. Naimi, Review of predictive maintenance algorithms applied to HVAC systems, Energy Rep. 8 (2022) 1003–1012.
[14] J. Chen, X. Gao, Y. Hu, Z. Zeng, Y. Liu, A meta-model-based optimization approach for fast and reliable calibration of building energy models, Energy 188 (2019), 116046.
[15] P. Raftery, M. Keane, A. Costa, Calibrating whole building energy models: detailed case study using hourly measured data, Energy Build. 43 (12) (2011) 3666–3679.
[16] G. Mustafaraj, D. Marini, A. Costa, M. Keane, Model calibration for building energy efficiency simulation, Appl. Energy 130 (2014) 72–85.
[17] M. Ahmad, C.H. Culp, Uncalibrated building energy simulation modeling results, HVAC R Res. 12 (4) (2006) 1141–1155.

[18] Z. Yang, B. Becerik-Gerber, A model calibration framework for simultaneous multi-level building energy simulation, Appl. Energy 149 (2015) 415–431.
[19] J.S. Haberl, D.E. Claridge, C. Culp, ASHRAE's Guideline 14-2002 for Measurement of Energy and Demand Savings: How to Determine what Was Really Saved by the Retrofit, 2005.
[20] I. Committee, International Performance Measurement and Verification Protocol: Concepts and Options for Determining Energy and Water Savings, vol. I, National Renewable Energy Lab., Golden, CO (US), 2001.
[21] M. V Femp, Guidelines: Measurement and Verification for Federal Energy Projects, Version 3.0," *Energy Effic*, Renew. Energy, 2008.
[22] D. Coakley, P. Raftery, M. Keane, A review of methods to match building energy simulation models to measured data, Renew. Sustain. Energy Rev. 37 (2014) 123–141.
[23] A. Cacabelos, P. Eguía, J.L. Míguez, E. Granada, M.E. Arce, Calibrated simulation of a public library HVAC system with a ground-source heat pump and a radiant floor using TRNSYS and GenOpt, Energy Build. 108 (2015) 114–126.
[24] J. Guo, R. Liu, T. Xia, S. Pouramini, Energy model calibration in an office building by an optimization-based method, Energy Rep. 7 (2021) 4397–4411.
[25] V.G. González, G.R. Ruiz, C.F. Bandera, Empirical and comparative validation for a building energy model calibration methodology, Sensors 20 (17) (2020).
[26] R.A. Lara, et al., Optimization tools for building energy model calibration, Energy Proc. 111 (2017) 1060–1069.
[27] D. Hou, I.G. Hassan, L. Wang, Review on building energy model calibration by Bayesian inference, Renew. Sustain. Energy Rev. 143 (2021), 110930.
[28] V. Martinez-Viol, E.M. Urbano, M. Delgado-Prieto, L. Romeral, Automatic model calibration for coupled HVAC and building dynamics using Modelica and Bayesian optimization, Build. Environ. (2022), 109693.
[29] S. Martínez-Mariño, P. Eguía-Oller, E. Granada-Álvarez, A. Erkoreka-González, Simulation and validation of indoor temperatures and relative humidity in multi-zone buildings under occupancy conditions using multi-objective calibration, Build. Environ. 200 (2021), 107973.
[30] P.E. Oller, J.M.A. Rodríguez, Á.S. González, E.A. Fariña, E.G. Álvarez, Improving the calibration of building simulation with interpolated weather datasets, Renew. Energy 122 (2018) 608–618.
[31] P. Raftery, M. Keane, J. O'Donnell, Calibrating whole building energy models: an evidence-based methodology, Energy Build. 43 (9) (2011) 2356–2364.
[32] D. Coakley, P. Raftery, P. Molloy, G. White, Calibration of a detailed BES model to measured data using an evidence-based analytical optimisation approach, Proc. Build. Simul. 2011 (2011).
[33] Y. Ji, P. Xu, A bottom-up and procedural calibration method for building energy simulation models based on hourly electricity submetering data, Energy 93 (2015) 2337–2350.
[34] G.Y. Yun, K. Song, Development of an automatic calibration method of a VRF energy model for the design of energy efficient buildings, Energy Build. 135 (2017) 156–165.
[35] Y.-S. Kim, M. Heidarinejad, M. Dahlhausen, J. Srebric, Building energy model calibration with schedules derived from electricity use data, Appl. Energy 190 (2017) 997–1007.
[36] S. Gopisetty, J. Pfafferott, Optimization of operational strategies for a low exergy office building, Energy Build. 60 (2013) 400–409.
[37] J. Pfafferott, S. Herkel, Statistical simulation of user behaviour in low-energy office buildings, Sol. Energy 81 (5) (2007) 676–682.
[38] N. Es-sakali, S. Idrissi Kaitouni, I. Ait Laasri, M.O. Mghazli, M. Cherkaoui, J. Pfafferott, Assessment of the energy efficiency for a building energy model using different glazing windows in a semi-arid climate, in: 2022 13th International Renewable Energy Congress, IREC), 2022, pp. 1–5, https://doi.org/10.1109/IREC56325.2022.10001934.
[39] S. Zuhaib, M. Hajdukiewicz, J. Goggins, Application of a staged automated calibration methodology to a partially-retrofitted university building energy model, J. Build. Eng. 26 (2019), 100866.
[40] M. Manfren, B. Nastasi, Parametric performance analysis and energy model calibration workflow integration—a scalable approach for buildings, Energies 13 (3) (2020) 621.
[41] J.E. Pachano, C.F. Bandera, Multi-step building energy model calibration process based on measured data, Energy Build. 252 (2021), 111380.
[42] N.R.M. Sakiyama, L. Mazzaferro, J.C. Carlo, T. Bejat, H. Garrecht, Natural ventilation potential from weather analyses and building simulation, Energy Build. 231 (2021), 110596.
[43] A. Cacabelos, P. Eguía, L. Febrero, E. Granada, Development of a new multi-stage building energy model calibration methodology and validation in a public library, Energy Build. 146 (2017) 182–199.
[44] B. Dong, Z. O'Neill, D. Luo, T. Bailey, Development and calibration of an online energy model for campus buildings, Energy Build. 76 (2014) 316–327.
[45] BIGLADDER, Number of timesteps per hour - input output references. https://bigladdersoftware.com/epx/docs/8-0/input-output-reference/page-006.html. (Accessed 18 April 2021).
[46] E. Burman, D. Mumovic, J. Kimpian, Towards measurement and verification of energy performance under the framework of the European directive for energy performance of buildings, Energy 77 (2014) 153–163.
[47] F. Ascione, N. Bianco, O. Böttcher, R. Kaltenbrunner, G.P. Vanoli, Net Zero-Energy Buildings in Germany: Design, Model Calibration and Lessons Learned from a Case-Study in Berlin, vol. 133, Energy Build., 2016, pp. 688–710.
[48] H. Mastouri, B. Benhamou, H. Hamdi, E. Mouyal, Thermal performance assessment of passive techniques integrated into a residential building in semi-arid climate, Energy Build. 143 (2017) 1–16.
[49] ASHRAE, ASHRAE standard 62.1. https://ashrae.iwrapper.com/ASHRAE_PREVIEW_ONLY_STANDARDS/STD_62.1_2019. (Accessed 8 February 2022).
[50] ASHRAE, ASHRAE standard 62.2. https://ashrae.iwrapper.com/ASHRAE_PREVIEW_ONLY_STANDARDS/STD_62.2_2019. (Accessed 8 February 2022).
[51] F.M. Baba, H. Ge, R. Zmeureanu, L.L. Wang, Calibration of building model based on indoor temperature for overheating assessment using genetic algorithm: methodology, evaluation criteria, and case study, Build. Environ. 207 (2022), 108518.
[52] ISO9869-1, International Standard Thermal Insulation — Building, 2014, pp. 1–11, 2014.
[53] ASTM C518, Standard Test Method for Steady-State Thermal Transmission Properties by Means of the Heat Flow Meter Apparatus, 2017, https://doi.org/10.1520/C0518-15.
[54] ISO8301, Thermal Insulation—Determination of Steady-State Thermal Resistance and Related Properties—Heat Fow Meter, 1997 [Online]. Available: https://cdn.standards.iteh.ai/samples/15421/899d628e428a4dfca34d3c78f74b7b76/SIST-ISO-8301-1997.pdf.
[55] DIN EN 12664, Thermal Performance of Building Materials and Products - Determination of Thermal Resistance by Means of Guarded Hot Plate and Heat Flow Meter Methods - Dry and Moist Products with Medium and Low Thermal Resistance, 2001. English ve. DIN, https://standards.globalspec.com/std/783856/DIN EN 12664.
[56] DIN EN 12667, Thermal Performance of Building Materials and Products - Determination of Thermal Resistance by Means of Guarded Hot Plate and Heat Flow Meter Methods - Products of High and Medium Thermal Resistance, 2001. English ve. DIN, https://standards.globalspec.com/std/841974/DIN EN 12667.
[57] M. Likins-White, R.C. Tenent, Z. Zhai, Degradation of insulating glass units: thermal performance, measurements and energy impacts, Buildings 13 (2) (2023) 551.
[58] ADTM, "Glass Check Pro. https://www.edtm.com/index.php/gc3001-glass-chek-pro. (Accessed 22 January 2022).
[59] WP4500, Energy Transmission Meter for Testing Operable Windows In-Frame, 2012. https://www.edtm.com/images/stories/pdf/manuals/WP4500_manual.pdf.
[60] EDTM, "Window Energy Profiler. https://www.edtm.com/index.php/wp4500-window-energy-profiler. (Accessed 14 October 2021).
[61] M. Royapoor, T. Roskilly, Building model calibration using energy and environmental data, Energy Build. 94 (2015) 109–120.
[62] A. Azouzoute, et al., Modeling and experimental investigation of dust effect on glass cover PV module with fixed and tracking system under semi-arid climate, Sol. Energy Mater. Sol. Cells 230 (2021), 111219.
[63] M. Abraim, et al., Techno-economic assessment of soiling losses in CSP and PV solar power plants: a case study for the semi-arid climate of Morocco, Energy Convers. Manag. 270 (2022), 116285.
[64] NSAI, "ISO 6946, The National Standards Authority of Ireland (NSAI) Produces the Following Categories of Formal Documents, 2017.

[65] D.G. Colliver, T.F. Burks, R.S. Gates, H. Zhang, Development of the Design Climatic Data for the 1997 ASHRAE Handbook–Fundamentals, Univ. of Kentucky, Lexington, KY (US), 2000.
[66] AMEE, Moroccan Thermal Regulation for Constructions, 2015. https://www.amee.ma/reglementation-thermique. (Accessed 13 December 2021).
[67] GREE, "Dc Inverter Multi Vrf System - Outdoor Units"..
[68] GREE, "Dc Inverter Multi Vrf System - Indoor Units"..
[69] R. Raustad, Creating Performance Curves for Variable Refrigerant Flow Heat Pumps in EnergyPlus, Florida Sol. Energy Cent., 2012.
[70] T. Kousksou, et al., Renewable energy potential and national policy directions for sustainable development in Morocco, Renew. Sustain. Energy Rev. 47 (2015) 46–57.
[71] N. El Asri, Y. Nouira, I. Maaroufi, A. Marfak, N. Saleh, M. Mharzi, The policy of energy management in public buildings procurements through the study of the process of delegated project management-Case of Morocco, Energy Pol. 165 (2022), 112944.
[72] R. Assadiki, F. Belmir, Current situation of green building development in Morocco: standards and certification systems, in: International Conference on Digital Technologies and Applications, 2022, pp. 563–572.
[73] Z. Romani, A. Draoui, F. Allard, Metamodeling the heating and cooling energy needs and simultaneous building envelope optimization for low energy building design in Morocco, Energy Build. 102 (2015) 139–148.
[74] S. Hamdaoui, M. Mahdaoui, A. Allouhi, R. El Alaiji, T. Kousksou, A. El Bouardi, Energy demand and environmental impact of various construction scenarios of an office building in Morocco, J. Clean. Prod. 188 (2018) 113–124.
[75] N. Abdou, Y.E.L. Mghouchi, S. Hamdaoui, N.E.L. Asri, M. Mouqallid, Multi-objective optimization of passive energy efficiency measures for net-zero energy building in Morocco, Build. Environ. 204 (2021), 108141.
[76] A. Benallel, A. Tilioua, A. Mellaikhafi, M.A.A. Hamdi, Thickness optimization of exterior wall insulation for different climatic regions in Morocco, Mater. Today Proc. 58 (2022) 1541–1548.
[77] J. Hou, D. Wei, X. Meng, B.J. Dewancker, Thermal performance analysis of lightweight building walls in different directions integrated with phase change materials (PCM), Case Stud. Therm. Eng. 40 (2022), 102536.